11th Australasian Fluid Mechanics Conference
University of Tasmania, Hobart, Australia
14-18 December 1992

THE COMPRESSIBLE TURBULENT BOUNDARY LAYER ON A STRONGLY HEATED WALL

Doug Bong LEE, Franck SOCHELAU and Roger LEBLANC

Laboratoire d'Etudes Aerodynamiques, CEAT
Universite de Poitiers, 86036 Poitiers Cedex, FRANCE

ABSTRACT

This paper concerns the theoretical and experimental modelling of the flat wall, highly heated, compressible turbulent boundary layer . Its final objective is to develop a numerical Navier-Stokes solver and to conclude on its capability to correctly represent the complex aerothermic viscous flows near the wall. The communication presents a costructed numerical method with particular attention given to the turbulence modelling at low Reynolds number and some selected experiments for the comparisons between the results. This comparison conducts to the first conclusion and gives some indications for the future works.

INTRODUCTION

Many aerospace engineering applications such as the compressible flows in turbines, scram jets, rockets, hypersonic configurations... are concerned with the aerothermic viscous flows. Basic experimental studies of the complex combination of the heat transfer and compressibility are required to understand their effects on the turbulent boundary layer characteristics. The results will be useful to build and to calibrate the numerical simulations of such fows. Due to the hypersonic applications, hot compressible turbulent boundary layer on cold wall is extensively analyzed. The present study considers the opposite situation of very hot wall heating a compressible turbulent boundary layer which was upstream in adiabatic equilibrium condition.

The objective of the present study is to develope an efficient boundary layer solver to calculate the aerothermic viscous flow on a strongly heated wall. The final objective is to predict more complex flows as for example shock / boundary layer interactions with heat and mass transfer. In such case, the present numerical method will be easily extended to calculate the Navier-Stokes equations.

The numerical method is presented in the next section. After a brief recall on the nature of governing equations, a low Reynolds number turbulence model as well as diverse topics on bounday layer calculation are considered. The selected experiments for comparison with the numerical results are presented in the following section. Supersonic data are due to ONERA (Office National d'Etudes et de Recherche Aérospatiales) whereas the transonic ones come from preliminary experiments recently conducted at CEAT (Centre d'Etudes Aérodynamiques et Thermiques). The comparisons between numerical and experimental results are made ,which indicate future works recommended in the conclusion.

NUMERICAL ANALYSIS

Governing Conservation Equations

The flows considered are assumed compressible (of variable density), steady and turbulent. A density weighting of the velocity and other dependent variables except pressure and, of course, density, so that these variables are decomposed into the sum of a density-weighted mean plus a corresponding fluctuation can be applied [1]. The conservation equations that result from this approach contain no density-fluctuation correlations, and are therefore analogous in appearance to those for incompressible flow. In the present study, the dependent variables are interpreted as density-weighted ones, and it is presumed that turbulence modelling practices which have been developed for incompressible flows are valid also for compressible flows and density-weighted averaging. The resulting statistically-averaged conservation equations of mass, momentum and energy are solved to obtain the pressure, velocity and temperature fields.

Turbulence Modelling

In direct analogy to laminar flows, turbulent transport is modelled using the Boussinesq stress-strain relation, which relates the Reynolds stress to the mean strain field by use of an isotropic eddy viscosity.

It is assumed that turbulence can be characterized by the turbulence kinetic energy (k) and the isotropic component of the turbulence energy dissipation rate (ϵ) which are determined from the transport equations. The turbulent viscosity is then calculated from the Prandtl-Kolmogorov formula.

Close to the wall, the local Reynolds number of turbulence is small and the molecular transport becomes important. To bridge the whole of the laminar sublayer to the fully turbulent region, the wall functions are used.

It has been found that this assumption cannot be valid within a laminar sublayer and appropriate functions must be chosen to ensure satisfactory predictions consistent with physical arguments. This is particularly important when there is a strong heat transfer at the wall. In this case the Reynolds number at the wall becomes very low and the laminar sublayer is so thick that the high Reynolds number calculation with wall function

may introduce important errors. Various proposals have been made to the low Reynolds number model. Patel et al. [2] evaluated some models. Among them, the models of Lam and Bremhorst [3] is chosen for the present study due to the following reasons. As the modification to the high Reynolds number model is only applied to the source term of the ϵ transport equation, this model can be very easily programmed without modifying the structure of the high Reynolds number model. The simplicity of the bounday conditions and favorable results of the test of Patel et al. are also those of the reasons.

Numerical Method

The numerical method employed to solve the governing equations is the one programmed in PHOENICS code [4]. In this numerical scheme, the flow equations are discretized using a finite-volume method on the staggered grid. To obtain velocity and pressure fields satisfying the mass and momentum conservation laws simultaneously, an iterative procedure called SIMPLEST is employed.

The boundary layer can be calculated either elliptically or parabolically. For the elliptic calculation the boundary condition at the far downstream position must be known as well as the initial profiles (upstream condition) and two boundary conditions (wall condition and free stream condition). The parabolic problem can be formulated only by neglecting the second derivative terms in the streamwise direction. The numerical scheme in PHOENICS is exactly the same for both the elliptic and parabolic case except that the influence from the downstream computational cell is neglected.

Details of the numerical problems as grid test, convergence criteria, generation of the initial profiles and calculation of the various boundary layer parameters are discussed in the CEAT internal note [5] and will be published later.

SELECTED EXPERIMENTS

Supersonic Boundary Layer

For present study, the ONERA experiments conducted in the S5Ch wind tunnel on heated supersonic boundary layer are used. The dimension of the test section is $300 \times 150mm^2$. The $400mm$ flat bottom wall is followed by a $510 \times 260 \times 30mm^3$ electrically heated plate. The stagnation conditions are atmospheric for the temperature and $0.75 \times 10^5 Pa$ for the pressure. Among the Mach numbers ($M_e = 2$;2.5; and 3) and the wall temperature ratios ($T_w/T_{wa} = 1.4$;1.6; and 2) experienced, the case $M = 2$, $T_w/T_{wa} = 2$ is presently considered for comparisons with the numerical modelling. These values require an electrical power of $12.75kW$ which gives a maximum surface temperature of $600°K$. The free stream unit Reynolds number is $0.5 \times 10^7/m$.

The heated wall pressure distributions are measured through 60 pressure holes and the wall temperature by 22 thermocouples embedded in the plate. Total pressure and temperature probes for the boundary layer survey pass through the plate and are supported by a step-motor carriage. More informations on the test set-up and its qualification and on the detailed measurements are given in the reference [6].

Transonic Boundary Layer

The experiments with transonic flow are conducted in the CEAT transonic wind tunnel which is of recirculating type: the dry air of the hypersonic ejector acting as an exhaust pipe is partly introduced in the settling chamber and accelerated through the nozzle at $M = 0.72$. The stagnation conditions are adjusted close to the atmospheric conditions and the unit Reynolds number is then $10^7/m$. A $0.6m$ flat plate, horizontally mounted from the settling chamber to the end of the $65 \times 85mm^2$ test section, separates the flow symmetrically. Its rear part, long of $0.1m$ and large of only $60mm$, contains the electrically heated plate thick of $8mm$. The $3kW$ installed power supply and the insulation of the plate lower side permit the upper surface temperature to reach $1150°K$. Then the value of the wall temperature ratio is $T_w/T_{wa} = 4$.

The flow fields are visualized by the schlieren method with a spark light source (time of exposure = $4\mu s$). Wall pressure distribution $p_w(x)$ are measured by holes of $\phi = 0.5mm$ situated on the symmetric axis of the upper test section wall. The wall temperature is measured by 3 thermocouples Cr-Al embedded in the plate. Static and total probes are positionned $10mm$ besides the flat plate axis of symmetry, at the x- distances selected for the boundary layer traverses. For the temperature measurements a Cr-Al thermocouple probe replaces the static pressure one.

The pitot and static pressure survey through the boundary layer along with a pressure recovery temperature measurement enable to draw the velocity and temperature profiles at the required stations along the plate. The pair of probes traverses the upper wall of the test section and are externally mounted on a motor-driven micrometer screw. Before each traverse a special attention is given to place precisely the probes at a desired y-position above the flat wall. Nevertheless, as mentionned below, the irregularities in the boundary layer integral quantities distributions will be attributed to that uncertainty. The step-motor is driven by a local PC which also perform the data acquisition. More details on the experimental procedure are given in the CEAT internal note [7]and will be published later.

COMPARISON OF THE RESULTS

Supersonic Boundary Layer

The supersonic boundary layer at $M_e = 2$ is calculated. The calculation begins 0.014 m upstream of the heating plate. The initial profiles are generated using the given experimental data. The three cases of wall heating are simulated such that: adiabatic wall (AD) or $T_{wa} = 307°K$ (ONERA experiment), heated wall (H2) or $T_w/T_{wa} = 2$ (ONERA experiment), and strongly heated wall (H4) or $T_w/T_{wa} = 4$ (no experimental result).

The velocity profile on the dimensional scale is presented in comparison with the experiment (Fig. 1). The calculated result accords well with the experiment eventhough the viscous diffusion is seen more active in the calculation.

The comparisons of numerical (solid line in the figures) and experimental integral quantities are presented by the following order: friction coefficient (experimental data are not available) (Fig. 2), and displacement thickness (comparison with experiment) (Fig. 3).

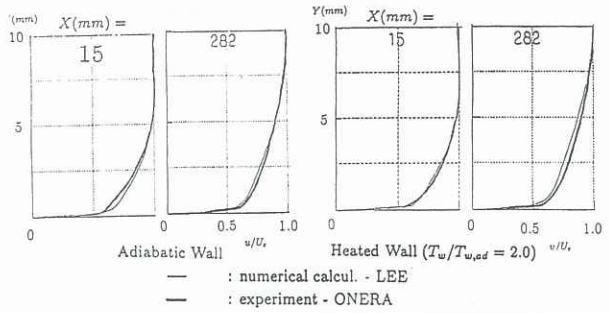

Figure 1: Velocity Profile (Exp. of ONERA)

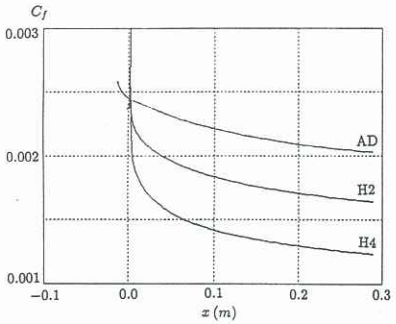

Figure 2: Friction Coefficient

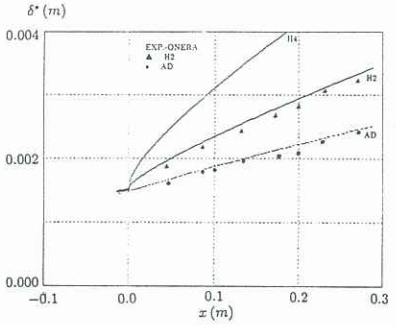

Figure 3: Displacement Thickness (Exp. of ONERA)

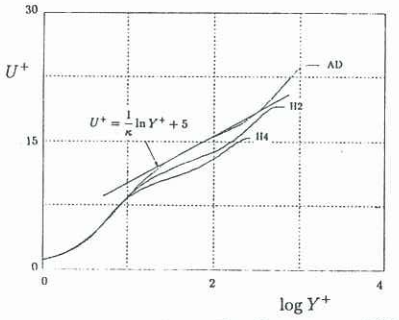

Figure 4: Velocity Log Law Profile at $x = 282mm$

One observes a discontinuity of the friction coefficient distribution at the junction of the adiabatic wall and the heated wall. This may be the result of the parabolic calculation of the bounday layer. One may explain the cause of this disconyinuity: by passing to the heated wall the velocity near the wall increases due to the expansion of the fluid volume and as a result the velocity gradient becomes higher than on the adiabatic wall. The molecular viscosity increases due to heating. These two increases (of velocity gradient and viscosity) result in the steep increase of the wall shear stress. After the discontinuity the friction coefficient diminishes with wall heating which provokes slower increase of the momentum thickness. The more remarkable wall heating effect is on the displacement thickness because the density is strongly influenced by temperature and as a result the mass flow rate per unit area (ρu) changes much.

Three velocity profiles (AD,H2 and H4) at the position of $x = 282\,mm$ are drawn on the log-law scale (Fig. 4). The adiabatic velocity profile fits well with the universal log law. Three remarks are made for the profiles on the heated wall: heating decreases the constant C of the log-law, wall heating reduces the log-law region, and wall heating does not influence the profiles in the sublayer region ($u^+ = y^+$).

Transonic Boundary Layer

The transsonic boundary layer at $M_e = 0.72$ is calculated. The calculation begins 0.70 m upstream of the heating plate. The two cases of wall heating are simulated such that: adiabatic wall (AD) or $T_{wa} = 275°K$ (CEAT experiment), strongly heated wall (H4) or $T_w/T_{wa} = 4$ (CEAT experiment).

The velocity profiles on the dimensional scale are presented in comparison with the experiment (Fig. 5). Only two profiles (one at the junction of the heating plate $x = 0mm$, the other at $80mm$ from the heating plate beginning) are presented here. The viscous diffusion effect is seen to be probably overestimated in the calculation and or the experimental boundary layer is not in the equilibrium state. As the velocity is deduced from the Mach number and temperature measurement using a probe recovery temperature, there is an accumulation of the errors from the three sources.

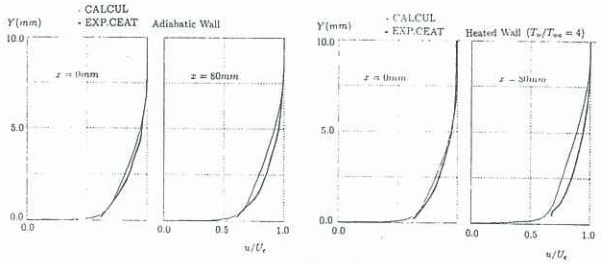

Figure 5: Velocity Profile (Exp. of CEAT)

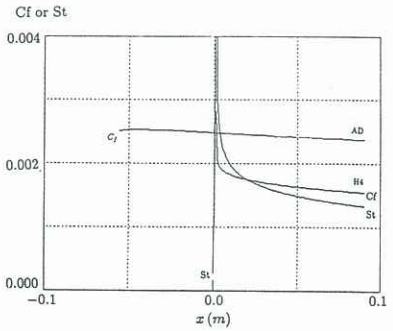

Figure 6: Friction Coefficient and Stanton Number (Exp. of CEAT)

The distributions of various boundary layer parameters are presented by the following order: friction coefficient and Stanton number (experimental data are not available) (Fig. 6), boundary layer thickness and displacement thickness (comparison with experiment) (Fig. 7), incompressible shape factor and shape factor (comparison with experiment) (Fig. 8), momentum thickness and total energy thickness (comparison with experiment)(Fig. 9).

We also observe a discontinuity of the friction coefficient distribution at the junction of the walls. Stanton

number at the wall junction edge is very high and after some distance it approaches to an equilibrium value. The high value of Stanton number at the beginning can be interpreted as a rapid increase of the total energy thickness (Fig. 9). The Reynolds analogy factor ($2St/C_f$) is not yet about the value of one. The thermal boundary layer is still in the developping state. The effect of the wall heating on the displacement thickness is more eminent for transonic boundary layer where the difference between the fluid temperature near the adiabatic wall and that on the heated wall is greater than the supersonic boundary layer for the same heating parameter ($H4$). Otherwise the behavior of the heated transonic boundary layer is very similar to its supersonic homologue. The incompressible shape factor increases with wall heating (the velocity profile becomes less full) but it seems that the difference between heated and adiabatic wall cases becomes smaller at the far downstream position.

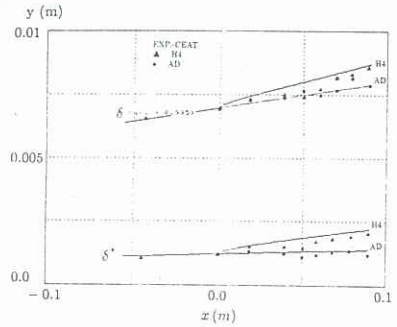

Figure 7: Boundary Layer Thickness and Displacement Thickness (Exp. of CEAT)

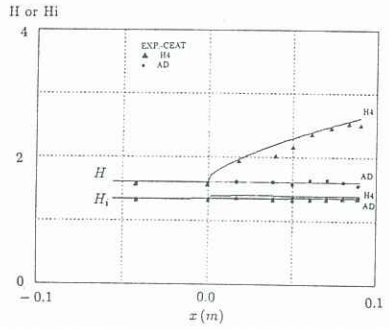

Figure 8: Incompressible Shape Factor and Shape Factor (Exp. of CEAT)

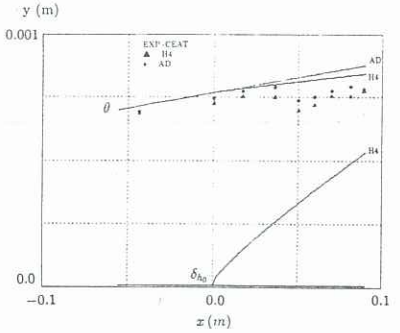

Figure 9: Momentum Thickness and Total Energy Thickness (Exp. of CEAT)

CONCLUSION AND FUTURE WORK

A numerical and experimental study is made to understand the behaviour of the compressible turbulent boundary layer on a strongly heated wall. For that purpose, a numerical method capable of calculating compressible turbulent flow with strong wall heat transfer is constructed. Also the measurements of a transonic turbulent boundary layer on strongly heated wall are realized. The conclusions obtained from the comparison of the both results indicate future ameliorations of the study:

- for the computation, studies of more elaborate turbulence model is required.
- for the experiment, methods of measurement near the heated wall is to be studied as well as the realization of boundary layer free from any experimental disturbances.

AKNOWLEDGEMENT

The first author, D.B. Lee, is a visiting professor to CEAT, on leave from Dept. of Mech. Eng., Inchon University, Inchon, Korea. This work was undertaken with the financial support of the Korean Science and Engineering Foundation (South Korea) and of the Centre National de la Recherche Scientifique (France) and with the agreement of Prof. Alziary de Roquefort, director of the Laboratoire d'Etudes Aéro-dynamiques. The PHOENICS codes was operated, in free access, in the Laboratoire d'Etudes Thermiques with the permission of Prof. Saunier, director, and of Dr. Bertin. The authors also acknowledge the help, during the present study, given by Mr. Ghayoub for the computations and by Mr. Garem for the experiments.

References

[1] Marvin, J G (1983) *Turbulence Modeling for Computational Aerodynamics.* AIAA J, 21, 941-955.

[2] Patel, V C , Rodi, W and Scheuerer G (1985) *A Review and Evaluation of Turbulence Models for Near Wall and Low Reynolds Number Flows.* AIAA J, 23, 1308-1319.

[3] Lam, C K G and Bremhorst K (1981) *A Modified Form of the $k-\epsilon$ Model for Predicting Wall Turbulence.* Trans. ASME, 103, 456 - 460.

[4] Rosten, H I and Spalding, D B (1991) *The PHOENICS Reference Manual.* CHAM TR/200, CHAM Limited, London.

[5] Lee, D B (1992) *Calculation of the turbulent boundary layer on a strongly heated wall.* Rapport Intern, CEAT/LEA URA 191, Université de Poitiers.

[6] Receveur, E and Salaün, M (1987) *Developpment d'une Couche Limite Turbulente Supersonique sur une Paroi Chauffée* . ONERA Rapport No. 71/7078 AY.

[7] Socheleau, F (1992) *Mesures preliminaires dans une couche limite turbulente compressible sur une paroi plane fortement chauffée.* DEA, CEAT/Université de Poitiers, en préparation.